



Automatic pectoral muscle boundary detection in mammograms based on Markov chain and active contour model*

Lei WANG[†], Miao-liang ZHU, Li-ping DENG, Xin YUAN^{†‡}

(School of Computer Science and Technology, Zhejiang University, Hangzhou 310027, China)

[†]E-mail: {thirtyking, yxxinyuan}@zju.edu.cn

Received Jan. 9, 2009; Revision accepted Mar. 2, 2009; Crosschecked Nov. 30, 2009

Abstract: Automatic pectoral muscle removal on medio-lateral oblique (MLO) view of mammogram is an essential step for many mammographic processing algorithms. However, it is still a very difficult task since the sizes, the shapes and the intensity contrasts of pectoral muscles change greatly from one MLO view to another. In this paper, we propose a novel method based on a discrete time Markov chain (DTMC) and an active contour model to automatically detect the pectoral muscle boundary. DTMC is used to model two important characteristics of the pectoral muscle edge, i.e., continuity and uncertainty. After obtaining a rough boundary, an active contour model is applied to refine the detection results. The experimental results on images from the Digital Database for Screening Mammography (DDSM) showed that our method can overcome many limitations of existing algorithms. The false positive (FP) and false negative (FN) pixel percentages are less than 5% in 77.5% mammograms. The detection precision of 91% meets the clinical requirement.

Key words: Pectoral muscle, Markov chain, Active contour, Mammogram

doi:10.1631/jzus.C0910025

Document code: A

CLC number: TP391.4

1 Introduction

Although there are progresses in other breast imaging modalities (magnetic resonance imaging, etc.), mammography is still the only viable clinical choice in detecting the early breast cancer, particularly for developing countries for years to come. Pectoral muscle removal on medio-lateral oblique (MLO) view of mammograms has been taken as an important preprocessing procedure in many mammographic processing methods. Yam *et al.* (2001) required the pectoral muscle present in the MLO view to be removed before reconstructing the breast in a 3D space. Timp *et al.* (2005) stated that their global registration method was improved when they excluded the pectoral muscle for determining the center-of-

mass. When a pectoral muscle is close to a mass boundary, the mass segmentation algorithm would fail (Dominguez and Nandi, 2007). Moreover, most breast density evaluation methods require the user to manually or semi-automatically segment pectoral muscle present in all MLO views (Glide-Hurst *et al.*, 2007).

In recent years, many automatic pectoral muscle boundary detection methods have been developed. As the sizes, the shapes and the intensity contrasts of pectoral muscles change greatly from one MLO view to another, no method can obtain precise muscle regions on all mammograms. Karssemeijer (1998) and Kinoshita *et al.* (2007) used one straight line obtained by Hough's and Radon's transform respectively to fit the pectoral muscle boundary. These methods produce huge errors when the pectoral muscle boundary is a curve (Fig. 1a). The inclusion tree based boundary detection method (Hong and Brady, 2003) is effective for mammograms on which the intensity contour of the muscle is quasi-concentric. But it produces wrong

[‡] Corresponding author

* Project (No. 60505009) supported by the National Natural Science Foundation of China

© Zhejiang University and Springer-Verlag Berlin Heidelberg 2010

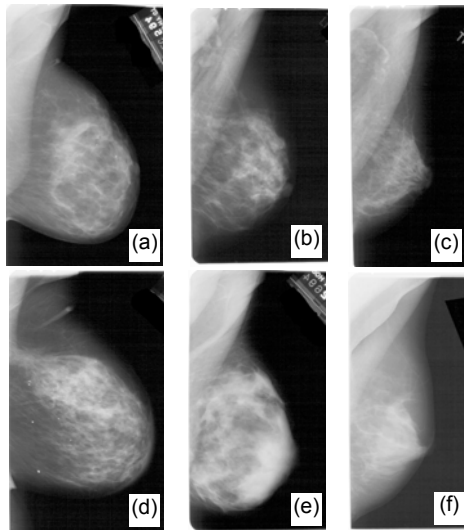


Fig. 1 Several mammograms on which pectoral muscle detection is difficult using existing algorithms

(a) Pectoral muscle boundary is a curve and becomes vertical in the lower part; (b) The intensities of the pectoral muscle change greatly; (c) The area of the pectoral muscle is larger than that of the breast; (d) The area of the pectoral muscle is very small and its boundary is nearly vertical in the lower part; (e) Pectoral muscle mixes in the glandular tissues in the lower part; (f) Pectoral muscle consists of several layers

detection results for mammograms on which the intensities in muscle region change greatly (Fig. 1b). Kwok *et al.* (2004) and Xu *et al.* (2007) searched pectoral muscle boundary in the pre-defined region of interest (ROI) using an iterative threshold and a mean square deviation method respectively. Selecting a suitable ROI, which impacts the final detection precision, is very difficult because the sizes of pectoral muscles change greatly from one mammogram to another (Figs. 1c and 1d). The Gabor wavelet based detection algorithm (Ferrari *et al.*, 2004) can obtain satisfactory results in detecting most pectoral muscle boundaries except those that are vertical or left tilting (Figs. 1a and 1d) because only the Gabor filters with 45° , 60° , and 75° response orientations are used in that algorithm to reduce the interferences caused by structures in muscles and glands. Graph theory based boundary detection methods (Bajger *et al.*, 2005; Ma *et al.*, 2007) concentrate only on the pixel intensities, which makes it difficult to distinguish pectoral muscles from adjacent glands when they have similar intensities (Fig. 1e). Carvalho *et al.* (2008) suggested a morphological closing operation to connect regions at the same gray level followed by using a morphological opening operation to obtain the pectoral mus-

cle region. This method may leave some pectoral muscles out especially when the muscle has several layers (Fig. 1f).

In this paper, we propose a novel boundary detection method based on a discrete time Markov chain (DTMC) and an active contour model. DTMC is used to obtain the rough boundary and the active contour model is applied to refine the detection results. As the method enables the capture of the stochastic nature of the boundary, it can overcome the limitations of existing algorithms.

2 Discrete time Markov chain

The Markov property is a conditional independence of the future evolution on the past (the whole history of the process being summarized in the current state). A random process is a collection of random variables indexed by the set I , taking values in the set S . DTMC is a random process with the Markov property whose index set (the time of Markov chain) and state space are discrete, either finite or countably infinite. Basically, the chain can be seen as modeling the position of an object in a discrete set of possible locations over time, and the next location being chosen at random from a distribution that depends only on the current one.

We define one-step transition probabilities as

$$p_{ij}^{(n-1)(n)} = P(X_n = j | X_{n-1} = i), \quad (1)$$

where $n \in I$, $i, j \in S$, X_n represents a random variable at time n . Then two-step transition probabilities can be calculated using one-step transition probabilities as follows:

$$p_{ij}^{(n-2)(n)} = \sum_{k \in S} p_{ik}^{(n-2)(n-1)} p_{kj}^{(n-1)(n)}. \quad (2)$$

Similarly, we can obtain n -step transition probabilities. Thus, if the initial distribution π^0 and one-step transition probabilities are determined, the probabilities of all states at any time can be obtained according to Eq. (3):

$$\pi_j^n = \sum_{i \in S} \pi_i^0 p_{ij}^{(0)(n)}, \quad (3)$$

where π_j^n denotes the probability in state j at time n .

3 Rough pectoral muscle boundary detection using DTMC

By analysis, we found two important characteristics of pectoral muscle boundary, i.e., continuity and uncertainty. As these two characteristics can be modeled using the Markov property and the probability of DTMC respectively, we considered using DTMC to detect the rough boundary of pectoral muscle.

In our rough boundary detection algorithm, state and time of DTMC correspond to the column and the row of the image respectively. Each row of the image is allocated to one random variable, which keeps the abscissa of the pectoral muscle boundary on the corresponding row. We set one row as the initial row and its random variable is X_0 . Then X_n is the variable whose corresponding row is n rows away from the initial row. To begin with, we build the initial distribution π^0 on the initial row and define one-step transition probabilities of DTMC. Then a rough boundary can be obtained by using the DTMC algorithm iteratively. After validation and correction operation, we obtain the final detection result.

3.1 Initial distribution and one-step transition probabilities

We choose one row, on which the pectoral muscle edge is relatively clear, as the initial row. Its ordinate y_{init} can be obtained using the following equation:

$$y_{init} = \max \left(y_{nar}, y_{top} + \frac{y_{wid} - y_{top}}{4} \right), \quad (4)$$

where y_{top} represents the ordinate of the breast's top edge, y_{wid} denotes the ordinate of the row with the widest breast width, and y_{nar} indicates the ordinate of the row with the narrowest breast width between y_{top} and y_{wid} . As the intensities near the initial row are similar inside the breast region and change greatly between the breast and pectoral muscle, finding the pectoral muscle edge on the initial row is relatively easy (Fig. 2a). We define

$$\text{Box}(x_0, y_0, \sigma) = \{(x, y) | x_0 - \sigma < x < x_0 + \sigma, y_0 - \sigma < y < y_0 + \sigma\}, \quad (5)$$

where x and y denote the abscissa and the ordinate of the point respectively, and σ is a constant. A scan line reflecting the pixels intensity fluctuation can be obtained by calculating the standard deviations of $\text{Box}(x, y, \sigma)$ for each point (x, y) along the initial row (Fig. 2b). After filtering the scan lines using a median filter, we pick up the rightmost peak satisfying Eq. (6):

$$L_{\text{peak}} - L_{\text{valley}} > \frac{\max(L) - \min(L)}{2}, \quad (6)$$

where L represents the values of all points on the scan lines, L_{peak} denotes the value of the peak on the scan line, and L_{valley} indicates the value of the valley right adjacent to the peak. The abscissa x_{init} corresponding to the peak is taken as the pectoral muscle edge on the initial row. Then, the initial distribution π^0 of the DTMC can be obtained using

$$\pi_i^0 = \begin{cases} 1, & \text{if } i=x_{init}, \\ 0, & \text{otherwise.} \end{cases} \quad (7)$$

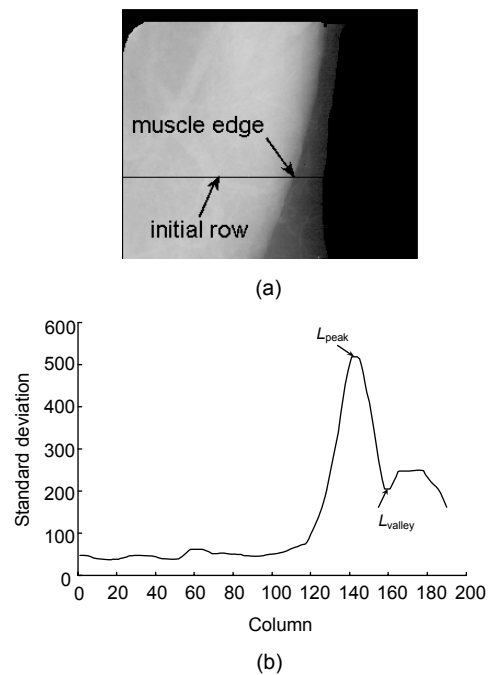


Fig. 2 Muscle edge detection on the initial row (a) The initial row; (b) The scan line along the initial row

The one-step transition probabilities can be calculated using the following equation:

$$P_{ij}^{(n-1)(n)} = \begin{cases} \frac{I_{\text{tran}}(j, y_n)}{\sum_{k=i-\gamma}^{i+\gamma} I_{\text{tran}}(k, y_n)}, & \text{if } |i-j| \leq \gamma, \\ 0, & \text{otherwise,} \end{cases} \quad (8)$$

where I_{tran} represents a 2D transition array and has the same size with the mammogram, $I_{\text{tran}}(x, y)$ denotes the value on the position (x, y) of the array, y_n indicates the ordinate of the row corresponding to the variable X_n , and γ is a constant used to control the transition distance of DTMC in one-step. Transition array I_{tran} changes during subsequent iterations and will be described in detail below.

3.2 Rough boundary detection

To minimize the time consumption of the detection algorithm, we define two regions of interest (ROIs) (Fig. 3a) as follows:

$$\begin{cases} \text{ROI}_1 = \{(x, y) | E_l \leq x \leq x_{\text{init}} + \mu, y_{\text{init}} \leq y \leq E_b\}, \\ \text{ROI}_2 = \{(x, y) | x_{\text{init}} - \mu \leq x \leq E_r, E_t \leq y \leq y_{\text{init}}\}, \end{cases} \quad (9)$$

where E_t , E_b , E_l , and E_r represent the top, bottom, left and right edges of the breast respectively, and μ is a constant. The right edge E_r of the breast is obtained by applying an adaptive thresholding method to the original mammogram, followed by smoothing the edge using chain codes. The detection algorithm can be described as follows:

Step 1: Create a 2D transition array I_{tran} by calculating the standard deviation of $\text{Box}(x, y, \sigma)$ for each points (x, y) in ROI_1 and ROI_2 (Fig. 3b).

Step 2: Initialize the iteration number as 0.

Step 3: While the iteration number is less than 3:

Step 3.1: Calculate the probabilities of the points in ROI_1 and ROI_2 using the DTMC (Eqs. (2) and (3)) based on the initial distribution π^0 and one-step transition probabilities, which can be obtained using Eqs. (7) and (8) respectively.

Step 3.2: Create a new I_{tran} . For the points in ROI_1 and ROI_2 , $I_{\text{tran}}(x, y)$ is equal to the probability of the point (x, y) obtained in Step 3.1. For other points, $I_{\text{tran}}(x, y)$ is 0 (Fig. 3c).

Step 3.3: The iteration number pluses 1.

Step 4: Pick up the point with the maximum value from each row of the latest I_{tran} to form the rough pectoral muscle boundary (Fig. 3d).

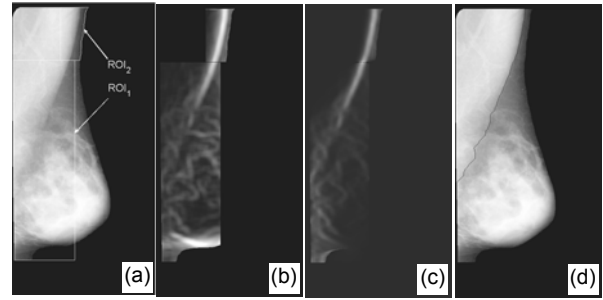


Fig. 3 Rough pectoral muscle detection

(a) The regions of interest; (b) I_{tran} created by calculating the standard deviation of $\text{Box}(x, y, \sigma)$ for each point (x, y) in ROI_1 and ROI_2 ; (c) I_{tran} created using probabilities after one iteration; (d) Detection result of rough pectoral muscle

For each row in I_{tran} , the larger one point's value is, the more likely the point is to be the boundary on this row. At the beginning of the iteration, many points have almost the same values on the rows with vague muscle boundary. Then the values of the points away from the boundary gradually decrease and those near the boundary increase with the iteration. An iteration number of 3 is chosen in Step 3 by experiments to strike a balance between processing time and accuracy.

3.3 Validation and correction

Our DTMC algorithm still has the chance to obtain the false pectoral muscle boundary at the lower part of the mammogram if the pectoral muscle mixes with the glandular tissues (Fig. 4a). To improve the detection precision, we validate the rough boundary and use a straight line to replace the false part.

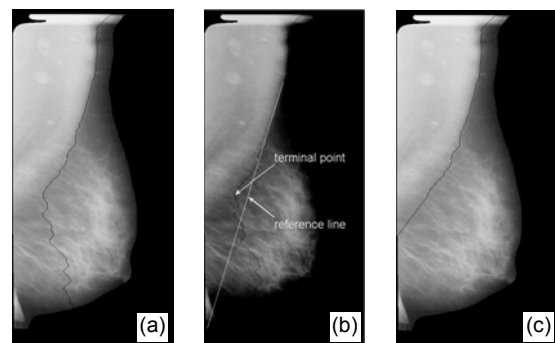


Fig. 4 Correction of the false part of the rough boundary

(a) Detection result of the DTMC algorithm (the rough boundary detected at the lower part of the mammogram is false because the pectoral muscle mixes in the glandular tissues); (b) Sketch map of correction; (c) The result after correction

According to prior knowledge, the intensities of pectoral muscle should be higher than those of fat and glandular tissues. Thus, for each row, if the summation of the intensities on the left side of the muscle edge is lower than that on the right side, the edge position on this row may be false. If there are too many false rows along the rough boundary, the boundary will be taken to be invalid. The number of false rows, N_{false} , can be calculated using the equation

$$N_{\text{false}} = \sum_{y=\Gamma_t}^{\Gamma_b} \text{sig} \left[\sum_{x=e_y}^{e_y+\varepsilon} I(x, y) - \sum_{x=e_y-\varepsilon}^{e_y} I(x, y) \right], \quad (10)$$

where Γ_t and Γ_b are the top and bottom ordinates of the rough boundary respectively, $I(x, y)$ represents the value of point (x, y) on the mammogram, e_y is the abscissa of the muscle edge on row y , ε is used to control the summary range and usually is a fixed number 20, and signature function $\text{sig}(x)$ is defined as

$$\text{sig}(x) = \begin{cases} 1, & \text{if } x > 0, \\ 0, & \text{otherwise.} \end{cases} \quad (11)$$

If $N_{\text{false}} > (E_b - E_t)/20$, where E_b and E_t are the bottom and top edges of the breast respectively, the rough boundary is invalid.

For an invalid boundary, we estimate a reference line from the point $(x_{\text{init}}, y_{\text{init}})$ to the left or bottom edge of the breast (Fig. 4b). The reference line's angle can be obtained using the equation

$$\theta_{\text{ref}} = \arctan \left[\xi^2 / \left(\sum_{y=y_{\text{init}}}^{y_{\text{init}}+\xi} e_y - \sum_{y=y_{\text{init}}-\xi}^{y_{\text{init}}} e_y \right) \right], \quad (12)$$

where e_y is the abscissa of the muscle edge on row y and ξ is a constant. Then the point on the rough boundary, which is on the left side of the reference line and has the maximum horizontal distance to it, is chosen as the terminal point (Fig. 4b). The boundary that is below the terminal point is considered to be false. Finally, we draw a straight line from the terminal point to the left or the bottom edge of breast to replace the false part of the boundary (Fig. 4c). The angle of the straight line can be obtained using the following equation:

$$\theta_{\text{replace}} = \arctan \frac{\xi}{e_{\text{tp}} - e_{\text{tp}-\xi}}, \quad (13)$$

where e_{tp} and $e_{\text{tp}-\xi}$ denote the abscissas of the rough boundary on the terminal point row and the row ξ lines above the terminal point, respectively.

4 Muscle boundary refinement

The muscle boundary detected using the DTMC algorithm is coarse because only local information (the transition probabilities between two adjacent rows) on the mammogram is used. Thus, we consider utilizing the global information, such as the boundary shape, to obtain a smooth and more precise pectoral muscle boundary. The active contour model is a suitable model for this purpose.

The traditional snake is an energy-minimizing spline under the influence of internal spline forces and image forces (Kass *et al.*, 2001). It works by moving through the spatial domain of an image to minimize the energy function

$$E = E_{\text{in}} + E_{\text{ex}}, \quad (14)$$

where E_{in} represents the internal energy used to control the snake shape, and E_{ex} denotes the external energy used to push the snake toward salient image features like lines and edges.

In our algorithm, we define the snake energy as

$$E = \int_{\Gamma_t}^{\Gamma_b} \left(\frac{1}{2} \alpha [e''(y)]^2 - I_{\text{tran}}(e(y), y) \right) dy, \quad (15)$$

where e denotes the rough pectoral muscle boundary and y is the ordinate, $e''(y)$ represents the second derivative of $e(y)$, Γ_t and Γ_b are the top and bottom ordinates of the boundary respectively, α is a weighted parameter that controls the snake rigidity, and I_{tran} is the 2D transition array used in the first iteration of the DTMC algorithm. The internal energy $\alpha[e''(y)]^2/2$ is used for obtaining a smooth pectoral muscle edge, and the external energy $I_{\text{tran}}(e(y), y)$ is to keep the total probabilities of the boundary as large as possible. The refinement results are shown in Fig. 5.

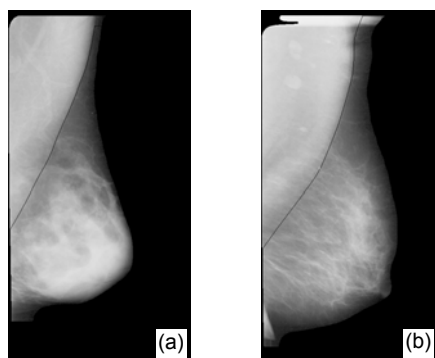


Fig. 5 Refinement results

(a) and (b) are refinement versions corresponding to Fig. 3d and Fig. 4c, respectively

5 Experimental results and discussions

Our detection algorithm was tested on the Digital Database for Screening Mammography (DDSM) (University of South Florida, 2001), supported by the Breast Cancer Research Program of the US Army Medical Research Material Command. A total of 200 MLO view mammograms were used in this paper. All images were scanned on either a Howtek 960 or a Howtek MultiRAD 850 digitizer with a sample rate of 43.5 microns at 12 bits/pixel. To reduce the time consumption of muscle boundary detection, all mammograms were down sampled to 800 pixels height.

Before pectoral muscle boundary detection, our algorithm would automatically judge the orientation of the mammograms and vertically mirror those in which the nipple faces to the left so that all pectoral muscles were at the top left corner of the images. Then an adaptive thresholding method was applied to eliminate the background with only breast and muscle remained. Finally, we used the algorithm introduced in this paper to detect the pectoral muscle boundary. The average processing time (not including the down sampling, orientation judging or thresholding) was 3.7 s for one mammogram on the computer with 2.0 GHz CPU, 512 MB memory and windows XP OS.

Table 1 shows the parameters used in our detection algorithm. h represents the height of the mammogram and is a fixed value 800 in this test. All parameters are determined by experiments. The principle to determine the parameter σ is to make the standard deviation of $\text{Box}(x, y, \sigma)$ large when point (x, y) is on the muscle boundary and small when it is on

other positions. The larger the parameter γ , the more likely the algorithm is to find the clear muscle boundary. However, large γ will produce false results for vague muscle boundary. To improve the algorithm efficiency, the parameter μ should be as small as possible in ensuring that two ROIs contain the total pectoral muscle boundary. Small ξ can increase the replace line's accuracy, but also has more chance to produce false replace lines. Large α produces straight and smooth boundary as it increases the weight of internal energy.

Table 1 Parameters used in our detection algorithm

Parameter	Value	Parameter	Value
σ	$h/80$	ξ	$h/20$
γ	$h/80$	α	0.05
μ	$h/80$		

σ : the range used to calculate the standard deviation; γ : the transition distance of DTMC in one step; μ : used to determine the size of the ROI; ξ : used in producing the reference line angle; α : a weighted parameter that controls the snake rigidity

To evaluate our experimental results, an experienced radiologist was invited to mark the reference pectoral muscle region on each mammogram manually. The segmented pectoral muscle region was defined as the left region enclosed by the breast border and the pectoral muscle boundary detected using our algorithm. Three evaluation criteria are used in this paper: false positive (FP) and false negative (FN) pixel percentages, the Hausdorff distance between the reference and the segmented pectoral muscle regions, and the mean distance from the boundary drawn by the radiologists to the closest point on the detected boundary.

We defined the FP pixel as the pixel outside the reference region that was included in the segmented region. Similarly, an FN pixel was defined as a pixel in the reference region that was not present within the segmented region. Then the FP and FN percentages could be calculated using the following equation:

$$\begin{cases} R_{fp} = N_{fp} / N_{ref} \times 100\%, \\ R_{fn} = N_{fn} / N_{ref} \times 100\%, \end{cases} \quad (16)$$

where N_{fp} and N_{fn} represent the FP and FN pixel numbers respectively, and N_{ref} is the number of pixels in the reference region. Good and acceptable

detection results were defined as those with R_{fp} and R_{fn} less than 5% and 10%, respectively.

Table 2 summarizes the FP and FN pixel percentages of our algorithm on all 200 mammograms. It can be seen that using the DTMC algorithm we can obtain 67.5% good results and 84% acceptable results in 200 mammograms. By using validation operation after the DTMC algorithm, the rates of the good and acceptable results raise to 75% and 91% respectively. Although the refinement operation can bring only 2.5% detection results from the acceptable group to the good group and seems invalid to unacceptable rough boundary, it increases the whole detection precision of the acceptable results, which can be observed from the mean column in Table 2. Errors in the unacceptable group are mainly caused by the muscle edge searching that fails on the initial row. The detected edge is more than 20 pixels away from the hand-drawn edge on the initial row in 13 out of totally 18 mammograms with unacceptable detection results. Therefore, developing a better algorithm for searching muscle edge on the initial row has a great chance to improve the final detection precision.

Table 2 FP and FN pixel percentages on 200 mammograms

Pixel percentage	Mammogram number			Mean (%)		
	I	II	III	I	II	III
$R_{fp} < 5\%$	80	87	88	1.17	1.23	0.09
$R_{fn} < 5\%$	55	63	67	2.81	2.98	1.37
$5\% \leq R_{fp} \leq 10\%$	13	8	4	7.91	8.16	6.64
$5\% \leq R_{fn} \leq 10\%$	20	24	23	8.42	9.10	7.06
$R_{fp} > 10\%$	27	10	10	67.25	87.42	93.23
$R_{fn} > 10\%$	5	8	8	27.40	24.86	22.47

Column I represents the results using only the DTMC algorithm, column II shows the results of rough pectoral muscle detection, and the final results are represented in column III

The Hausdorff distance $H(A, B)$ is defined as

$$H(A, B) = \max(h(A, B), h(B, A)), \quad (17)$$

where A and B represent the sets of the pixels in the reference muscle region and segmented muscle region respectively,

$$h(A, B) = \max_{a \in A} \min_{b \in B} \|a - b\|, \quad (18)$$

and $\|\cdot\|$ is the Euclidean distance. The mean distance $MD(A, B)$ used in this paper is defined as

$$MD(A, B) = \frac{1}{N} \sum_{n=1}^N \min_{b \in B} \|a_n - b\|, \quad a_n \in A, \quad (19)$$

where A and B represent the pixel sets of the boundary drawn by the radiologist and the detected boundary respectively, N is the number of pixels on the boundary drawn by the radiologist. Table 3 illustrates the Hausdorff distance and the mean distance of our algorithm on all 200 mammograms.

Table 3 Hausdorff distance and mean distance on 200 mammograms

	Distance (pixels)	Mammogram number
Hausdorff distance, H	$H \leq 5$	97
	$5 < H \leq 10$	56
	$10 < H \leq 20$	22
	$H > 20$	25
Mean distance, MD	$MD \leq 5$	174
	$5 < MD \leq 10$	8
	$10 < MD \leq 20$	3
	$MD > 20$	15

As the test data, the radiologists and the evaluation criteria are different in existing papers, it is unreasonable to directly compare detection results among different algorithms. Fig. 6 shows some final detection results using our algorithm.

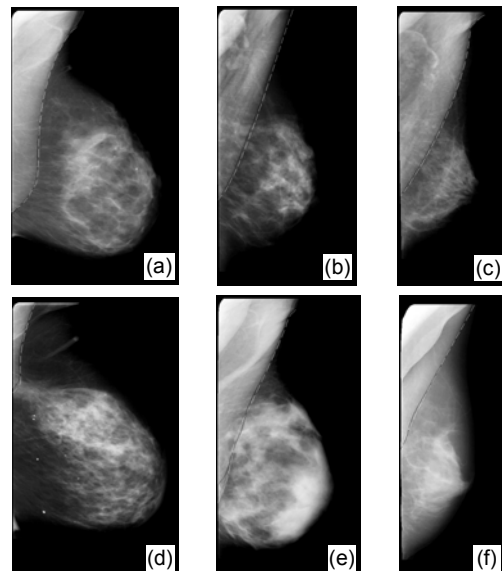


Fig. 6 Some muscle boundary detection results using our algorithm

(a)–(f) are corresponding to the mammograms in Fig. 1. Black lines represent the boundaries detected by our algorithm and white dashed lines are the boundaries drawn by the radiologist

6 Conclusion

In this paper, we propose a new method based on DTMC and an active contour model to automatically detect the pectoral muscle boundary on mammograms. The method can overcome the limitations of many existing muscle detection algorithms by taking advantage of the continuity and uncertainty of the muscle boundary and combining the local and global information. Experimental results on images from DDSM showed that our method is effective for most mammograms. The DTMC algorithm proposed in this paper seems effective in detecting the edges with continuity and uncertainty properties and can be used in other applications. In the future, we will focus on improving the searching precision of the muscle edge on the initial row and combining other useful features to create the 2D transition array.

References

- Bajger, M., Ma, F., Bottema, M.J., 2005. Minimum Spanning Trees and Active Contours for Identification of the Pectoral Muscle in Screening Mammograms. Proc. Digital Image Computing Techniques and Applications, p.323-329. [doi:10.1109/DICTA.2005.55]
- Dominguez, A.R., Nandi, A.K., 2007. Improved dynamic-programming-based algorithms for segmentation of masses in mammograms. *Med. Phys.*, **34**(11):4256-4269. [doi:10.1118/1.2791034]
- Ferrari, R.J., Rangayyan, R.M., Desautels, J.E.L., Borges, R.A., Frere, A.F., 2004. Automatic identification of the pectoral muscle in mammograms. *IEEE Trans. Med. Imag.*, **23**(2):232-245. [doi:10.1109/TMI.2003.823062]
- Glide-Hurst, C.K., Duric, N., Littrup, P., 2007. A new method for quantitative analysis of mammographic density. *Med. Phys.*, **34**(11):4491-4498. [doi:10.1118/1.2789407]
- Hong, B.W., Brady, M., 2003. A Topographic Representation for Mammogram Segmentation. *Medical Image Computing and Computer-Assisted Intervention*, p.730-737. [doi:10.1007/b93811]
- Karssemeijer, N., 1998. Automated classification of parenchymal patterns in mammograms. *Phys. Med. Biol.*, **43**(2):365-378. [doi:10.1088/0031-9155/43/2/011]
- Kass, M., Witkin, A., Terzopoulos, D., 1988. Snakes: active contour models. *Int. J. Comput. Vis.*, **1**(4):321-331. [doi:10.1007/BF00133570]
- Kinoshita, S., Azevedo-Marques, P., Pereira, R., Rodrigues, J., Rangayyan, R., 2007. Radon-domain detection of the nipple and the pectoral muscle in mammograms. *J. Dig. Imag.*, **21**(1):37-49. [doi:10.1007/s10278-007-9035-6]
- Kwok, S.M., Chandrasekhar, R., Attikiouzel, Y., Rickard, M.T., 2004. Automatic pectoral muscle segmentation on mediolateral oblique view mammograms. *IEEE Trans. Med. Imag.*, **23**(9):1129-1140. [doi:10.1109/TMI.2004.830529]
- Ma, F., Bajger, M., Slavotinek, J.P., Bottema, M.J., 2007. Two graph theory based methods for identifying the pectoral muscle in mammograms. *Pattern Recogn.*, **40**(9):2592-2602. [doi:10.1016/j.patcog.2006.12.011]
- Timp, S., van Engeland, S., Karssemeijer, N., 2005. A regional registration method to find corresponding mass lesions in temporal mammogram pairs. *Med. Phys.*, **32**(8):2629-2638. [doi:10.1118/1.1984323]
- University of South Florida, 2001. Digital Database for Screening Mammography. Available from <http://marathon.csee.usf.edu/Mammography/Database.html> [Accessed on Jan. 9, 2005].
- Xu, W.D., Li, L.H., Liu, W., 2007. A Novel Pectoral Muscle Segmentation Algorithm Based on Polyline Fitting and Elastic Thread Approaching. Proc. 1st Int. Conf. on Bioinformatics and Biomedical Engineering, p.837-840. [doi:10.1109/ICBBE.2007.218]
- Yam, M., Brady, M., Highnam, R., Behrenbruch, C., English, R., Kita, Y., 2001. Three-dimensional reconstruction of microcalcification clusters from two mammographic views. *IEEE Trans. Med. Imag.*, **20**(6):479-489. [doi:10.1109/42.929614]